

Thickness-Dependent Electronic Structure of Intermetallic CeCo₂ Nanoribbon Films Studied by X-ray Absorption Spectroscopy

Chung-Li Dong,[†] Chi-Liang Chen,[†] Kandasami Asokan,^{*,‡} Ching-Lin Chang,[§] Yang-Yuan Chen,[†] Jyh-Fu Lee,^{||} and Jinghua Guo[⊥]

[†]Institute of Physics, Academia Sinica, Taipei 11529, Taiwan, Republic of China, [‡]Inter-University Accelerator Centre, Aruna Asaf Ali Marg, New Delhi-110067, India, [§]Department of Physics, Tamkang University, Tamsui 251, Taiwan, Republic of China, ^{||}National Synchrotron Radiation Research Center, Hsinchu, Taiwan, Republic of China, and [⊥]Advanced Light Source, Lawrence Berkeley National Laboratory, Berkeley, California 94720

Received November 24, 2008. Revised Manuscript Received May 1, 2009

We report the electronic structure study of intermetallic CeCo₂ nanoribbon films of various thicknesses by X-ray absorption near-edge structure (XANES) spectroscopy at Ce L₃-, Co K-, and L_{2,3}-edges. The Ce L₃-edge absorption spectra reveal that the contribution of tetravalent Ce component increases with the film thickness, and all investigated nanoribbon films exhibit intermediate valence nature. Variation of the spectral intensities observed at the Co K-edge threshold implies modification in the Co 3d states and the enhancement of 3d-4f-5d hybridization. The Co 3d and Ce 4f occupation numbers were estimated from these spectroscopic results. The present study brings out how the surface-to-bulk ratio and the charge transfer between Ce and Co ions affect the electronic structure of nanoribbon films.

1. Introduction

Nanometer scale thin films (or nanoribbon films) of thickness from 10 to a few hundred nanometers are of great interest for understanding fundamental questions such as how surface properties develop into bulk properties and how their electronic structure modifies during the process of such change over. Among rare-earth-based intermetallics, cerium (Ce)-based compounds fascinate materials scientists because of their puzzling electronic properties such as kondo effects, long-range magnetic ordering, coexistence of heavy-fermionic behavior, and superconductivity.¹ These unusual properties are commonly attributed to hybridization of the 4f electrons with the conduction electrons. Most Ce compounds in their stable trivalent state, [Xe] 4f¹ configuration, show antiferromagnetic ordering at low temperature, and only a few compounds show ferromagnetic ordering. CeCo₂ is a superconducting compound with transition temperature T_c of 1 K.¹ It is considered that the Ce in CeCo₂ is in the intermediate valence state due to the collapsed volume.^{1–3} Its extremely low magnetic susceptibility indicates that both Ce and Co ions are essentially nonmagnetic in this compound.^{1,4} The intriguing behavior of 4f electrons in rare-earth compounds is that it can possess both localized and band-like nature, giving rise to the extraordinary magnetic and electronic properties. The electronic or magnetic properties of nanostructured materials are different from those of the bulk, even for the same chemical composition and stoichiometry. This is attributed to either the quantum size effect that increases the lowest unoccupied states and lowers the highest occupied electronic state, or the nonquantum size effect such as the structure disorder or surface

reorganization. A recent study on the heavy fermion compound CeAl₂ has demonstrated that the bulk CeAl₂ exhibits magnetic ordering, while the nanoparticles of the same compound show nonmagnetic nature.⁵ This phenomenon has been attributed to the variation in the Ce 4f electronic configuration resulting from the different surface-to-bulk ratio.⁶ On the other hand, bulk CeCo₂ is characterized as a Pauli paramagnet, and it undergoes a nonmagnetic–magnetic transition with size reduction down to the nanoscale.⁴ From the previous specific heat study,⁵ the linear coefficient of specific heat γ was 150 mJ/mol K² for the bulk CeAl₂ and became 9000 mJ/mol K² in CeAl₂ nanoparticles of 9.8 nm. A significant enhancement of the Kondo behavior is also accompanied by a decreased Kondo temperature T_K (from 5 K to 0.5 K). In contrast, the γ was about 37 mJ/mol K² for bulk CeCo₂, and the γ increased to 350 mJ/mol K² with $T_K \sim 0.4$ K.^{7,8} Since the linear coefficient of specific heat γ is proportional to the electron density of states (DOS),^{5,9} the change of γ will give rise to the different electronic configuration. Thus CeCo₂ exhibits much weaker behavior compared to CeAl₂.^{4,5}

X-ray absorption near-edge structure (XANES) provides direct information on valency and depicts the transition from core level to unoccupied electronic states near the Fermi level (E_F). Hence it is a preferred experimental tool to study the modulation of the electronic structure of films of nanometer thickness. XANES can probe the charge transfer and the change in local electronic structure of atoms or preferred occupation sites around a specific atom. Hence, one would expect a significant difference in the XANES spectra of CeAl₂ and

*Corresponding author. E-mail: asokan@iuac.res.in

(1) Allen, J. W.; Oh, S.-J.; Lindau, I.; Maple, M. B.; Suassuna, J. F.; Hagstrom, S. B. *Phys. Rev. B* **1982**, *26*, 445.

(2) Lawrence, J. M.; Riseborough, P. S.; Parks, R. D. *Rep. Prog. Phys.* **1981**, *44*, 1.

(3) Allen, J. W.; Oh, S. J.; Gunnarsson, O.; Schönhammer, K.; Maple, M. B.; Torikachvili, M. S. *Adv. Phys.* **1986**, *35*, 275.

(4) Wang, C. R.; Chen, Y. Y.; Yao, Y. D.; Chang, C. L.; Weng, Y. S.; Wang, C. Y. *J. Magn. Magn. Mater.* **2002**, *239*, 524.

(5) Chen, Y. Y.; Yao, Y. D.; Wang, C. R.; Li, W. H.; Chang, C. L.; Lee, T. K.; Hong, T. M.; Ho, J. C.; Pan, S. F. *Phys. Rev. Lett.* **2000**, *84*, 4990.

(6) Chang, C. L.; Dong, C. L.; Huang, C. L.; Chen, Y. Y. *J. Appl. Phys.* **2000**, *87*, 3349.

(7) Chen, Y. Y.; Jang, S.-J.; Wang, C. R.; Yang, H. D. *Physica B* **2005**, *359–361*, 497.

(8) Chen, Y. Y.; Wang, C. R.; Yao, Y. D.; Ou, M. N.; Chen, B. J. *Phys. Rev. Lett.*, submitted for publication.

(9) Chen, Y. Y.; Yao, Y. D.; Hsiao, S. S.; Jen, S. U.; Lin, B. T.; Lin, H. M.; Tung, C. Y. *Phys. Rev. B* **1995**, *52*, 9364.

CeCo₂: a single-peak profile in the case of CeAl₂ and double-peak profile for CeCo₂ that arise primarily as a result of the difference in their electronic configurations.

2. Experimental Details

The bulk CeCo₂ sample was prepared by the arc-melting method from high-purity constituent elements Ce (99.95%) and Co (99.95%) in 1:2 atomic ratios in an argon atmosphere (99.999%). In order to obtain a homogeneous phase of CeCo₂, melting was repeated five times and annealed at 900 °C for a week. The CeCo₂ nanothin films of thickness 30, 40, 75, 110, and 140 nm were fabricated on to a glass substrate without cooling by flash evaporation of bulk CeCo₂ ingot. All the “as-prepared” nanothin films were annealed at 900 °C for the duration of 1 week. The structure and phase purity were determined by X-ray diffraction, and these films were found to be in cubic Laves structure with a lattice constant of $a_0 = 7.160 \text{ \AA}$.

X-ray absorption measurements were performed at the National Synchrotron Radiation Research Center (NSRRC), Taiwan. The XANES spectra at Ce L₃- and Co K-edges were carried out at Wiggler beamline 17C using fluorescent mode at room temperature. The monochromator Si (111) crystals were used at Wiggler beamline 17C with an energy resolution $\Delta E/E$ better than 2×10^{-4} . The energy resolution at 5723 eV (Ce L₃-edge) was about 0.3 eV, and for the Co K-edge, it was $\sim 0.4 \text{ eV}$. In order to eliminate the effect of the self-absorption, all measurements were done in normal incidence geometry. Since pure Ce gets oxidized very easily, the energy scale was calibrated by using vanadium thin film (V K-edge at 5465 eV). The Ce L₃-edge has an absorption energy of 5723 eV, which is $\sim 160 \text{ eV}$ above the V K-edge. The compound CeF₃ was used as a reference for the Ce L₃-edge, which shows a single peak profile at 5727.1 eV. Apart from this, the experimental setup allows one to simultaneously measure the reference sample CeF₃ behind the CeCo₂ nanothin films. The signal of this reference sample was noisy because of the X-rays that can not totally transverse the substrate. However, the first-differential point of raising absorption edge still allowed us to check the energy. The XANES spectra at Co L_{2,3}-edges were recorded at HSGM beamline 20A using total electron yield mode. The energy resolution was set to 0.2 eV.

3. Results and Discussion

Figure 1 shows Ce L₃-edge XANES spectra of CeCo₂ nanothin films along with bulk CeCo₂. The large number of unoccupied Ce 5d orbitals, via 2p to 5d transition, results in two prominent L₃ white lines, marked as A₁ and B₁. The ground state of the Ce atom has the electronic configuration of [Xe] 4f¹5d¹6s². In Ce intermetallics, the 5d¹6s² electrons participate in bonding and form a part of the valence band. The 4f electron occupancy is primarily determined by the chemical environment. This can be visualized as two configurations, 4f¹ (Ce³⁺ state) and 4f⁰ (Ce⁴⁺ state), which result in two distinct spectral structures (A₁ and B₁) in Ce L₃-edge XANES. The double-peak spectral shape at the L₃-edge is known to be the signature of the *intermediate valence* nature.^{10,11} In general, Ce L₃-edges of strongly correlated systems, such as cerium-based oxides, display three characteristic contributions associated with 4f¹, 4f⁰L, and 4f⁰ configurations when Ce ions are in +3 and +4 states. For such systems, there is strong hybridization of the Ce states with O 2p states, which give rise to ligand holes represented

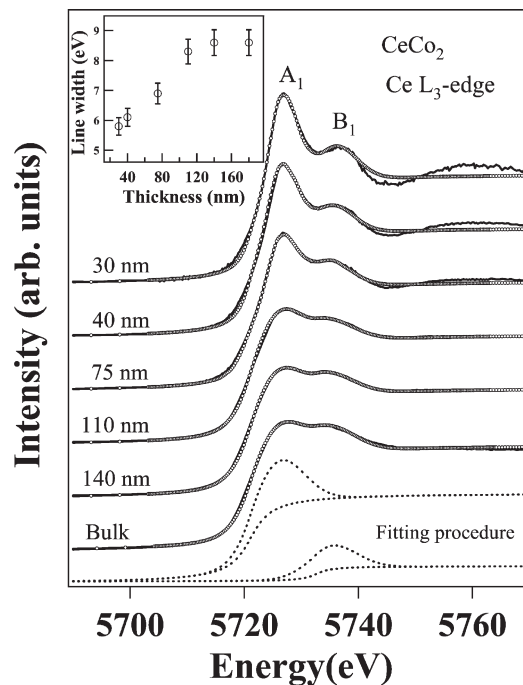


Figure 1. XANES spectra at Ce L₃-edge for bulk and various thicknesses of CeCo₂ nanothin films. Note the change in spectral features A₁ and B₁ with the thickness of the film. Inset shows the line-width of spectral feature A₁ which changes with the film thickness.

as 4f⁰L configurations.^{12,13} As to the intermetallic compound, CeCo₂, the ligand hole state is absent and should result in two contributions at the threshold of the Ce L₃-edge spectra. The inset shows the profile of the line-width of the spectral feature A₁ and the thickness of the nanothin films. As evident from Figure 1, there is a clear spectral evolution indicating a change in the valency and line-widths depending on film thickness. These parameters are likely to provide better understanding of the intermetallics. Enhancement of the 4f¹ state implies an increase of 4f electron occupancy at Ce site as the thickness decreases. In Figure 1, all spectra show trivalent and tetravalent Ce valence states as shown in the fitting procedure (deconvoluted) marked by dashed lines at the bottom of the figure. Each valence state can be decomposed into a Gaussian function and an arctangent edge jump function.¹⁴ The former function describes the localized 5d final states, which reflect the Ce³⁺ or Ce⁴⁺ valence states, and the latter represents the transition to continuum states above E_f . The open circles represent the fitting curve by summing the weighted Ce³⁺ and Ce⁴⁺. The fitting curves are found to be in good agreement with the experimental results. Subsequently, the average valency of Ce was evaluated by following a standard procedure,¹⁵ $\bar{v} = 3 + (I_{Ce^{4+}} / (I_{Ce^{3+}} + I_{Ce^{4+}}))$, where $I_{Ce^{3+}}$ and $I_{Ce^{4+}}$ are associated with the integrated intensities of the trivalent and tetravalent Ce contributions. The estimated valencies of Ce for bulk, 140, 110, 70, 40, and 30 nm nanothin films are, respectively, 3.30, 3.30, 3.28, 3.27, 3.24, and 3.22. It clearly shows that the valency increases with thickness of nanothin films. There is minor a discrepancy

(10) Le Fèvre, P.; Magnan, H.; Hricovini, K.; Chandresis, D.; Vogel, J.; Formoso, V.; Eickhoff, T.; Drube, W. *Phys. Status Solidi B* **1999**, *215*, 617.

(11) Chaboy, J.; Piquer, C.; García, L. M.; Bartolomé, F.; Wada, H.; Maruyama, H.; Kawamura, N. *Phys. Rev. B* **2000**, *62*, 468.

(12) Lee, C. H.; Oyanagi, H.; Sekine, C.; Shirovani, I.; Ishii, M. *Phys. Rev. B* **1999**, *60*, 13253.

(13) Soldatov, A. V.; Ivanchenko, T. S.; Della Longa, S.; Kotani, A.; Iwamoto, Y.; Bianconi, A. *Phys. Rev.* **1994**, *B50*, 5074.

(14) Röhrler, J.; Mang, J. *Magn. Mater.* **1985**, *47&48*, 175.

(15) Lee, C. H.; Oyanagi, H.; Sekine, C.; Shirovani, I.; Ishii, M. *Phys. Rev. B* **1999**, *60*, 13253.

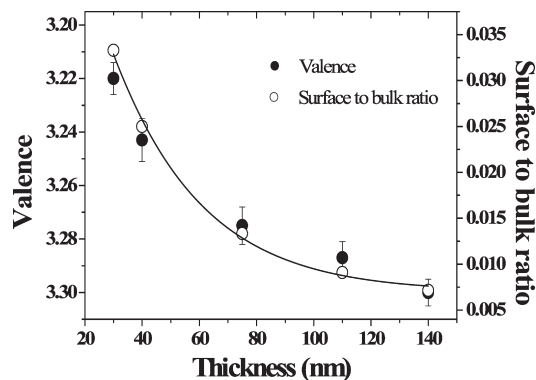


Figure 2. Ce valency variation and surface-to-bulk ratio with thickness.

from the fitting around 5720 eV due to the contribution of the dipole-forbidden 2p to 4f transitions.

Two major factors determine the electron energy levels in nanoscale materials: the increased surface area, and the reduced coordination number. The former broadens the band, while the latter tends to narrow the band.¹⁶ The band narrowing is observed in Ce L₃-edge XANES as the thickness is decreased (shown in the inset of Figure 1), indicating the reduced coordination number. This observation is also consistent with results of CeAl₂ thin films and CeCo₂ nanoparticles.¹⁷ In CeAl₂ nanoparticles, the valency change is explained by the stronger surface pressure lifting the 4f level up close to the conduction band.⁶ However, the present result does not support this statement since there is no shift of the Ce 4f levels relative to the E_f, otherwise the valency should enhance as the thickness of the CeCo₂ thin film is increased. Apparently, in addition to the modification of the Ce 4f level position due to the increase of the valency, there should be other competing mechanisms that dominate the valency change in the CeCo₂ system.

The physical and chemical properties of solid-state matter are determined primarily by the bulk volume. In the case of nanomaterials, these properties could be influenced significantly by the surface area. The surface-to-volume ratio is a useful parameter when studying the transition from bulk to nanomaterials. Surface tension (γ) and cohesive energy (G) are two important physical quantities that determine the growth and thermal stability of the materials. While surface tension is caused by the attraction between the molecules due to various intermolecular forces, the bulk cohesion is the energy required to separate the atoms of the solid into isolated atomic species. Since γ refers to the surface energy per unit area and G is the attractive energy per unit volume, one can represent the surface energy as γA and the bulk cohesive energy as GV where the quantities A and V represent the surface area and volume of the solid, respectively. In nature, materials attempt to balance surface energy and bulk cohesive energy (i.e., $\gamma A = GV$). Thus the surface-to-bulk ratio is defined as the ratio of the number of surface atoms to the number of bulk atoms and reflects the relative magnitude between the surface tension and bulk cohesive energy of the material. In other words, the surface-to-bulk ratio directly refers to the surface-to-bulk energy ratio ($A/V = G/\gamma$) and is inversely proportional to the radius or thickness of the solid if the shape has a perfect geometry. The analysis of the surface-to-bulk

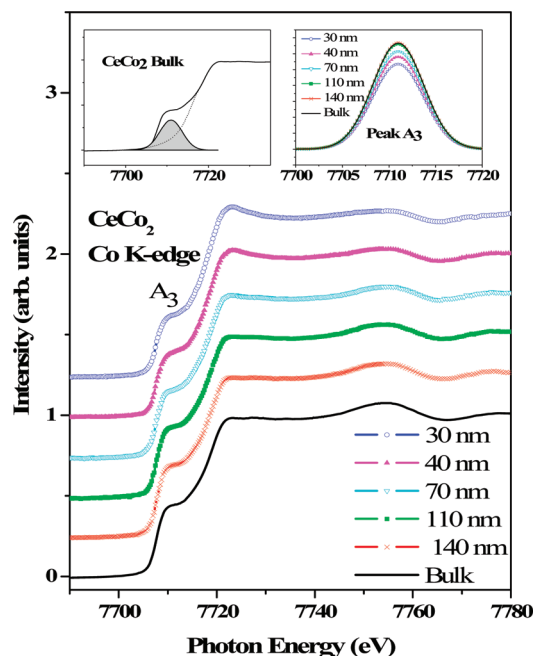


Figure 3. XANES spectra at Co K-edge for bulk and nanofilms of CeCo₂. Inset demonstrates the change of the shoulder-like feature A₃ after subtracting the background.

ratio is useful in understanding the electronic structures of these nanofilms. The dimensions of the nanofilm films in this study were $\sim 5 \text{ mm} \times 5 \text{ mm} \times \text{thickness}$. The surface layer is about few atomic monolayers, and it is assumed that the thickness of surface layer is d . Thus the surface area should be regarded as a very thin layer of $\sim 5 \text{ mm} \times 5 \text{ mm} \times d$. If the contribution of the side wall of the film is neglected, the surface-to-bulk ratio is solely determined by the ratio of $\text{layer}_{\text{surface}}/\text{layer}_{\text{total}}$, and thus the surface-to-bulk ratio results as $\sim d/\text{thickness}$. Consequently, the thickness plays an important role in the surface-to-bulk ratio of nanofilm films, and the values of surface-to-bulk ratio are estimated to be 0.0333, 0.0251, 0.0133, 0.0091, and 0.0071 for 30, 40, 75, 110, and 140 nm, respectively. These results along with the valency as a function of thickness are shown in Figure 2. This analysis of surface-to-bulk ratio appears to be adequate. In short, for solids, the physical and chemical properties of solids are determined by the bulk, and, for nanofilm films, the properties are influenced primarily by the surface.

To understand the origin of variation of Ce valency and the correlation at the Co site, we measured XANES at Co K- and L_{2,3}-edges. Taking advantage of the orbital and site selectivity offered by X-ray absorption process, by tuning the photon energy near Co K- and L_{2,3}-edges, one can investigate the electronic structure at the Co site and valency change. The normalized XANES spectra at the Co K-edge are presented in Figure 3. For Co K-edge absorption, where the inner 1s electron is excited to the final state, the 4p orbital reflects the density of unoccupied 4p states above the Fermi level, thus the Co K-edge mainly probes the unoccupied 4p states. However, the pre-edge peak structure is attributed to 3d character due to the hybridized Co 4sp-Co 3d states as well as the hybridized Ce 4f-5d-Co 3d states.¹⁸ As a result, the prepeak comprises mixed states, and its intensity does not directly reflect the change of the Co 3d state alone.

(16) Mason, M. G.; Lee, S.-T.; Apai, G.; Davis, R. F.; Shirley, D. A.; Franciosi, A.; Weaver, J. H. *Phys. Rev. Lett.* **1981**, *47*, 730.

(17) Dong, C. L.; Asokan, K.; Chang, C. L.; Chen, C. L.; Chen, Y. Y.; Lee, J. F.; Guo, J.-H. *J. Electron Spectrosc. Relat. Phenom.* **2006**, *152*, 1.

(18) Sham, T. K.; Hiraya, A.; Watanabe, M. *Phys. Rev. B* **1997**, *55*, 7585.

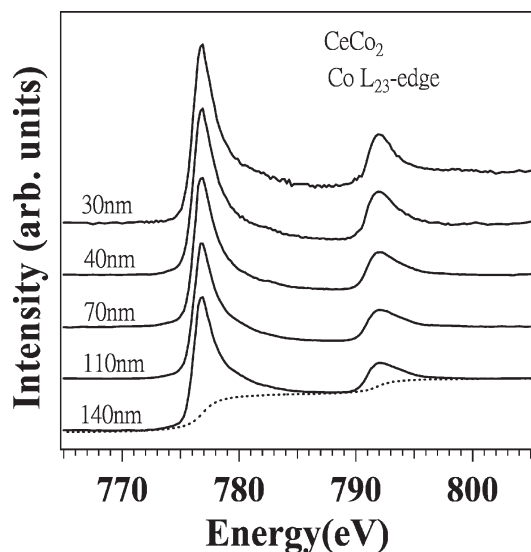


Figure 4. XANES spectra at Co $L_{2,3}$ -edges for various $CeCo_2$ nanofilm thicknesses. The intensity of spectral features increases as thickness of the film decreases.

Inset (left) in Figure 3 displays how the shoulder feature A_3 is deduced from the curve fitting using Lorentzian function after the background subtraction. The right inset shows A_3 intensity dependence upon the changing of film thickness. Calculations of ref 19 and 20 indicate that the spectral feature A_3 arises from the stronger hybridization between the conduction states of Ce (4f, 5d) and those of Co (3d).^{19,20} Thus, the modification of A_3 may reflect the change of the hybridization strength and variation of the density of empty 3d states.²¹ This systematic reduction in the intensity of the feature A_3 with decreasing thickness results from a reduced hybridization between conduction states of Ce (4f, 5d) and of the corresponding Co 3d states. A progressive decreased intensity also implies the change in the Co 3d states resulting from the electronic perturbation of the DOS driven by the surface-to-bulk ratio.¹¹ Band structure calculations show that the DOS near the E_f largely arises from the Ce 4f band and Co 3d band. This calculation further reveals that the contributions to the DOS at E_f from Co 3d, Ce 4f, and Ce 5d states are about 45, 31, and 7%, respectively.²² The other contributions are substantially small.

To evaluate the change of Co 3d states precisely, we measured the XANES spectra at Co $L_{2,3}$ -edges that probe the transition from 2p to 3d states and give direct information about the unoccupied 3d states. Figure 4 shows the normalized XANES spectra at the Co $L_{2,3}$ -edge. The integrated intensity across the absorption edge after removing the transition to the continuum states (marked by the dashed line) is proportional to the density of unoccupied 3d states. Since there is a strong correlation between these unoccupied 3d states and the 3d occupancy, one would use this fact to understand the above results. The ground-state configuration of Co metal is $3d^7$. The ground state configuration for the complete “3d occupancy” is $3d^{10}$. So it becomes more convenient to count the “unoccupied 3d states”

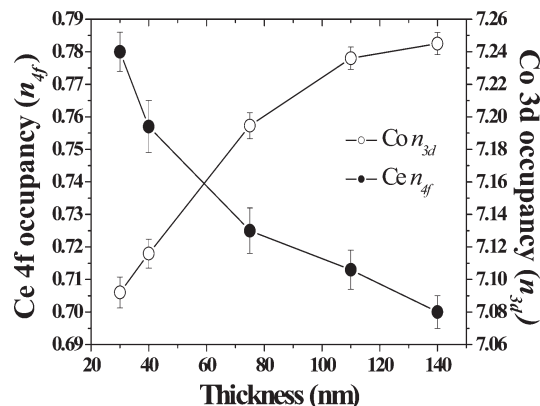


Figure 5. The graph shows the occupancy of Ce 4f and Co 3d at different thickness.

using the parameter of “3d occupancy”. One would start with Co metal and bulk $CeCo_2$ and assume their 3d occupancy numbers to be 7 (Co) and 7.5 (bulk $CeCo_2$).^{23–25} The area under XANES spectra was measured to be 13.9 and 7.9, respectively, for Co metal and bulk $CeCo_2$. Since the area under the XANES spectra is proportional to the unoccupied state, the 3d occupancy can be estimated.^{24,25} Thus, the estimated “3d occupancy” will be 7.093, 7.116, 7.195, 7.237, and 7.245 for nanofilm thicknesses of 30, 40, 75, 110, and 140 nm, respectively.

This is plotted in Figure 5 along with the occupancy number of Ce. The Ce 4f occupancy numbers can be translated from the valency, which is estimated from Figure 1, by $n_f = 4 - v$. It shows that the occupation of the Co 3d states decreases with a corresponding increased Ce 4f occupation as the thickness reduces. It is noted that the variation of Ce 4f occupancy is about ~11%, and the estimated variation of 3d occupancy is about ~5%. If one takes account of the Co ions atomic ratio in $CeCo_2$, the variation of Co 3d occupancy is consistent with that of Ce 4f occupancy. This experimental observation suggests there is charge transfer between Ce and Co, thus the charge transfer is another factor in addition to the surface effect that influences the Ce valency.

When the thickness of $CeCo_2$ film decreases, the relatively reduced hybridization and charge transfer results in less charge distribution in the 3d orbital. As a result, the 3d band moves up toward the E_f .^{26,27} This is consistent with the recent calculation that predicts that the 3d band of surface Co atom becomes narrower and pushed up slightly toward the E_f in comparison with the bulk.²⁸ As the band is pushed toward the E_f , the hybridization should be increased without affecting the Ce 4f levels. However, this argument conflicts with the XANES result, which shows small hybridization in thinner nanofilms. Consequently, the influence of the Ce site has to be taken into account. Possible explanations are that (i) the narrowing of Ce 4f band,²⁹ in accordance with the result from the line-width shown in Figure 1, or (ii) the shift of the 4f band away from the E_f may reduce the

(23) Panfilov, A. S.; Grechnev, G. E.; Svechkarev, I. V.; Sugawara, H.; Sato, H.; Eriksson, O. *Physica B* **2002**, *319*, 268.

(24) Hsieh, H. H.; Chang, Y. K.; Pong, W. F.; Pieh, J. Y.; Tseng, P. K.; Sham, T. K.; Coulthard, I.; Naftel, S. J.; Lee, J. F.; Chung, S. C.; Tsang, K. L. *Phys. Rev. B* **1998**, *57*, 15204.

(25) Naftel, S. J.; Bzowski, A.; Sham, T. K. *J. Alloy Compd.* **1995**, *283*, 5.

(26) Severin, L.; Johansson, B. *Phys. Rev. B* **1994**, *50*, 17886.

(27) Dong, C. L.; Chen, Y. Y.; Chen, C. L.; Asokan, K.; Chen, C. L.; Liu, Y. S.; Chen, J. L.; Lee, J. F.; Guo, J.-H. *Phys. Status Solidi B* **2007**, *244*, 4526.

(28) Guo, G. Y.; Wang, Y. K.; Chen, Y. Y.; Wang, J. J. *Magn. Mater.* **2004**, *272–276*, e1193.

(29) Jarlborg, T.; Freeman, A. J.; Koelling, D. D. *J. Magn. Magn. Mater.* **1986**, *60*, 291.

(19) Eriksson, O.; Nordstrom, L.; Brooks, M. S. S.; Johansson, B. *Phys. Rev. Lett.* **1988**, *60*, 2523.

(20) Duo, L.; Vavassori, P.; Braicovich, L.; Olcese, C. L. *Phys. Rev. B* **1995**, *51*, 4751.

(21) Bianconi, A. In *X-ray Absorption: Principles, Applications, Techniques of EXAFS, SEXAFS and XANES*; Koningsberger, D.C., Prins, R., Eds.; Wiley: New York, 1988.

(22) Aoki, Y.; Nishigaki, T.; Sugawara, H.; Sato, H. *Phys. Rev. B* **1997**, *55*, 2768.

overlap of the 3d and 4f bands.²⁸ The band structure calculations, based on generalized gradient approximation (GGA) in pseudopotential and GGA with the on-site Coulomb energy U (GGA + U) calculation shows the Ce 4f states from the surface layer is shifted away from the E_f by 2 eV. Thus, even though the 3d band is shifted up to the E_f , the overlap of wave function from 3d and 4f decreases and also reduces hybridization strength in nanothin films. From the above discussion, the valency change is closely related to the surface-to-bulk ratio, and the charge transfer between Ce and Co has the consequence of the valency change driven by the different surface-to-bulk ratio.

4. Conclusion

The XANES study at the Ce L₃-edge revealed that Ce ions are in the *intermediate valence state*, and the contribution of the

tetravalent component increases as the thickness of the CeCo₂ nanothin films increases. XANES at Co K- and L_{2,3}-edges show that the hybridization strength and 3d occupancy also varies with film thickness. It is found that charge transfer from Ce to Co increases with thickness of CeCo₂ nanothin films. Both the bulk-to-surface effect and the presence of Co 3d charge transfer modify the Ce 4f electron occupation, resulting in the change of DOS and the valency. The experimental findings suggest that the valency change in CeCo₂ is due to the charge transfer driven by the surface-to-bulk ratio effect.

Acknowledgment. This work was supported by the National Science Council of the Republic of China through Grant Number NSC 95-2112-M-032-008, and the U.S. Department of Energy, under Contract No. DE-AC02-05CH11231.